Adaptive Master-Slave Unscented Kalman Filter for Grid Voltage Frequency Estimation

Juan P. Muñoz [1], Mario E. Magaña [2*], Eduardo Cotilla-Sanchez [2]

[1] Intel Corporation, Hillsboro, Oregon, USA
[2] School of EECS, Oregon State University, Corvallis, Oregon, USA
[*] corresponding.author@second.com

Abstract: **The frequency of the grid voltage is a time-varying parameter caused by mismatches between power generation and power consumption. In fact, the fundamental frequency decreases when large loads are connected to the system or when a large generation source goes offline. The opposite holds true for an increase in the fundamental frequency e.g. when generation exceeds consumption. Hence, in order to protect a power system against loss of synchronism, under-frequency relaying, and power system stabilization, accurate frequency estimation is necessary.**
This paper proposes an adaptive algorithm based on a master-slave unscented Kalman filter (MS-UKF) configuration to estimate both the voltage frequency and the measurement noise. Specifically, the master UKF uses the strong tracking filter (STF) condition to improve tracking accuracy, speed of convergence, and to desensitize the filter from initial conditions. The slave UKF uses the master UKF innovation to estimate the measurement noise covariance. Our approach addresses the tracking weaknesses of other frequency estimation algorithms when the frequency of the grid voltage waveform changes abruptly. Algorithm performance is measured through computer simulation.

1. Introduction

Variations in generation, demand, and other factors result in compromised quality of the supply grid voltage. For this reason, accurate frequency estimation in a power system is necessary to maintain a high level of quality. Specifically, frequency estimation is used for protection against loss of synchronism, under-frequency relaying, and power system stabilization [1, 2].

The frequency of the grid voltage is a parameter whose changes are caused by mismatches between power generation and power consumption [3]. Generally, frequency variations occur when a generator that is isolated from the grid is supplying power to the loads [4]. Also, as explained in [4], the fundamental frequency decreases when large loads are connected to the system or when a large generation source goes offline. The opposite holds true for an increase in the fundamental frequency (e.g. generation exceeds consumption).

Current research work in sustainable energy systems is aimed at tackling this frequency estimation problem, but many challenges still remain [5]. For example, renewable energy sources like solar energy or wind turbines are more likely to exhibit frequency variations due to frequent mismatch between power supply and demand. Further discussion regarding the importance of frequency estimation in the smart grid can be found in [5].

Traditionally, the frequency of a sinusoidal signal corrupted with noise is estimated using the time between two zero crossings and the calculation of the number of cycles [6-8]. To estimate the frequency, the authors in [6] use the minimum observation time for a given error or the minimum error for a given observation time, for a given signal-top-noise ratio as the performance criterion. A sample count and interpolation technique augmented by a three consecutive sample refinement is proposed in [7]. In [8] a non-iterative method that uses four data points in an arbitrary fixed time interval is used to estimate the frequency. In all these cases, the sinusoid does not undergo changes of the fundamental frequency and the algorithms are not robust with respect to the observation noise. In other words, they are not appropriate to estimate the frequency when the signal undergoes transient or abnormal changes, such as those experienced by the power grid voltage/current signals. In order to overcome this disadvantage, alternative methods have been proposed. For example, Fast Fourier Transform (FFT)-based algorithms are presented in [9-11]. In [9] the authors present a technique which uses a bandpass filter and three DFT/IDFT samples recursively to estimate the frequency. Reference [10] proposes a hybrid frequency estimation algorithm based on a second-order Taylor series expansion and a Fourier-based algorithm. Although these last two algorithms can estimate dynamic changes in the frequency, they are applied to a noise-free model. Recently, the authors in [11] proposed to estimate the frequency of a noisy, though undistorted sinusoidal signal in two steps. In the first step, a coarse estimate is made by the position of the maximum DFT amplitude and in the second step the estimate is refined by using the amplitude of two DFT coefficients. Another popular frequency estimation approach is least squares (LS) [12-15]. In [12] a least mean squares technique in complex form with variable adaptation step-size is proposed to compute the frequency of three-phase voltages which are represented in complex form. The algorithm is able to follow smooth changes in frequency, but has a hard time tracking step changes. In [13] the author presents a hybrid LS algorithm to estimate the fundamental frequency of a noisy sinusoid which may contain some harmonics. Specifically, the signal is first filtered to remove its DC component and then an LS-based that uses four points is applied. The algorithm is not applied to cases where the frequency undergoes rapid changes. The authors in [14] present a complex-valued LS algorithm to estimate the frequency of unbalanced three-phase voltages. To obtain

the frequency estimate, the authors first obtain three time series relationships among equidistantly spaced Clarke's [14] transformed voltage samples and then apply a complex-valued LS algorithm to reduce the effect of noise and harmonics. The authors only test their algorithm when voltages undergo amplitude variations without drastic changes in frequency. In [15] the authors present a nonlinear LS algorithm to estimate the frequency of a noise-free sinusoidal signal. According to their simulation results, the algorithm takes too long to track step changes in frequency, even in the absence of noise. A modified Prony-based estimation algorithm to track voltage variations is presented in [16]. The frequency estimation is performed using a filter bank, so that the order of the transfer polynomial used by the Prony's method can be reduced substantially. This methods works well when the variations of the waveforms are associated with the amplitude only.

Newer frequency estimation variants are proposed in [17-19]. In [17] the authors present a dynamic model based frequency estimation with step change detection algorithm. To detect the step changes in the signal, this algorithm first obtains the derivative from the short-time Fourier transform and the first-order Taylor series expansion of the phasor model. The frequency is estimated using a higher-order Taylor series expansion model that represents the dynamic characteristics of the signal. The algorithm works well for step changes in the amplitude but the authors do not show any results with drastic changes in the fundamental frequency of the sinusoid. In [18], the authors propose an algorithm based on the DFT and three digital filters to reduce the estimation errors due to noise and the leakage effect. Specifically, the algorithm estimates the frequency from the magnitude ratios of DFT coefficients to avoid the leakage effect. The frequency tracking of this approach is good for smooth changes in the frequency, but does not track very well step changes in the frequency. In [19] the authors estimate the frequency of an undistorted, albeit noisy sinusoid by first filtering the signal with two orthogonal FIR filters and then using three consecutive samples from each subband. Although the algorithm is sufficiently fast for online estimation, it does not have the capability of estimating fast time varying frequencies.

Recently, a widely linear adaptive frequency estimation algorithm for unbalanced three-phase power systems was proposed in [20]. Their approach is the complex-valued extension of the iterative version of the complex LMS algorithm. Although this method tracks changes in frequency due to voltage sags, it does not achieve steady-state convergence.

When a model that describes the time evolution of the state of a dynamic process and a model of noisy state measurements exist along with their prior and posterior probability distributions, Bayesian estimation can be applied to dynamic state estimation [21]. Furthermore, when both dynamic state and measurement models are linear and the process and measurement noises are Gaussian distributed, the Kalman Filter is the optimum state estimator [22]. When either the state dynamic model or the measurement model or both are nonlinear, suboptimal Bayesian nonlinear filters such as extended Kalman filters, unscented Kalman filters and particle filters can be designed to estimate the states. The presence of nonlinearities does not permit the propagation over time of the Gaussian statistics. To deal with this problem, the EKF uses local linearization to approximate the prior probability distribution as Gaussian. Similarly, the UKF uses the unscented transform to preserve the Gaussian property of the prior distribution, although the UKF can still produce good estimates when the statistics are not Gaussian. Particle filters (PF), on the other hand, are sequential Monte Carlo methods based on "particle" representations of probability density functions which can be applied to any state-space model and generalize KF methods [21]. Although PFs are more general than KF variants, they are all based on the concept of sequential importance sampling (SIS) by drawing samples from an importance density function [21]. Moreover, they represent the required posterior density function by a set of random samples with associated weights which are used to compute the estimates. When the number of samples is large, the PF estimates approach the optimal Bayesian estimates. PFs, however, suffer from the problem of degeneracy [21] and a large computational effort is needed to minimize it by using the concept of resampling.

When the process dynamics are well known and the process noise is adequately chosen, the EKF and the UKF produce smaller estimation errors than the PF [23]. Furthermore, the PF is very sensitive to the value of the process noise and the estimation errors increase [23]. For estimation problems where the nonlinearities are described by abrupt changes, the EKF performs poorly and the UKF and the PF perform better. Although the authors in [24] obtained comparable mean squared estimation errors for all three dynamic estimators, they found that the computational complexity of the PF was significantly higher than that of both EKF and UKF (it is almost the same for both EKF and UKF). Specifically, the authors in [24] found that the computational complexity of the PF was between 37 and 137 times that of the EKF and the UKF. This is due to the use of Monte Carlo sampling and resampling by the PF.

Bayesian dynamic estimation of frequency has been recently applied using the Kalman filter and its variants [25-29]. In [25] the authors present a linear Kalman filter to detect fast modal changes in power systems, including frequency estimation. In [25] the frequency is estimated via differentiation of the phase angle which does not undergo abrupt changes. In [26] an extended Kalman filter and a sliding-surface-enhanced fuzzy adaptive controller technique is used to estimate the frequency of power systems. Although this approach achieves a relatively good steady-state tracking, it has difficulties tracking the frequency during a long period of time after an abrupt change in frequency occurs. In [27] a fourth-order unscented Kalman filter is used to track both frequency and amplitude variations of a distorted power signal corrupted by noise. This implementation tracks amplitude changes fairly well, but does not do a very good job tracking abrupt changes in frequency. Regulski *et al*. [29] present an unscented Kalman filter to estimate frequency and power components using a fourth-order power signal model rather than a voltage signal model. This approach can estimate the changes in power components very well but has difficulties tracking the frequency.

In this paper we present a new adaptive frequency estimation algorithm based on the UKF [27] for three-phase voltage signals found in power systems. The algorithm is adaptive in the sense that the measurement (observation)

variance is estimated on-line. Specifically, we propose an estimation configuration with feedback where the frequency is estimated by a (master) UKF in the forward path and the variance of the measurement noise is estimated by another (slave) UKF in the feedback path which uses the innovation information generated by the master UKF as its input. Because of the substantially higher computational complexity of the PF in relation to the UKF and the fact that the complex-valued nonlinear voltage dynamics can be analytically described, we choose the proposed master-slave UKF (MS-UKF) algorithm and apply the strong tracking filter (STF) condition [30-31] to improve the speed of convergence and tracking capabilities whenever large and abrupt frequency changes occur and the statistics of the measurement noise are unknown. The STF condition is also applied for the purpose of decreasing the sensitivity to initial conditions.

The rest of the paper is organized as follows: In section 2 the signal model and state-space representation of the three-phase grid voltage waveform are presented first, then in section 3 the proposed adaptive MS-UKF design is described. Section 4 evaluates system performance via computer simulation. Section 5 presents the concluding remarks.

2. Signal model and state-space representation

Several linear and nonlinear models have been proposed to estimate the grid voltage frequency, phase, and amplitude of a single sinusoid [5-12]. This paper uses a complex-valued state-space representation for the signal model of a three-phase power system. This complex-valued representation is much simpler and direct when dealing with frequency estimation.

Assuming a balanced system, the discrete-time representation of the three phase voltages of a power system is given by

$$\begin{aligned} V_{a_k} &= V_m \cos\left(\theta(kT)\right) + v_{a_k} \\ V_{b_k} &= V_m \cos\left(\theta(kT) - \frac{2\pi}{3}\right) + v_{b_k}, \\ V_{c_k} &= V_m \cos\left(\theta(kT) + \frac{2\pi}{3}\right) + v_{c_k} \end{aligned} \tag{1}$$

where the parameters V_m, $\theta(t)$, and T are the peak amplitude of the fundamental component, the time-varying phase angle, and the sampling period, respectively. The terms v_{a_k}, v_{b_k}, and v_{c_k} are noise terms associated with the measurements and are defined as independent and identically distributed white Gaussian random variables with zero mean and variance σ^2.

The discretised time-varying phase angle is defined as

$$\theta(kT) = \int_0^{kT} \omega(\tau)d\tau + \phi, \tag{2}$$

where $\omega(t)$ is the time-varying radian/s frequency and ϕ is a fixed phase angle.

It is possible to represent all three phases as a single signal in complex form by means of the $\alpha\beta$-transform [20]

$$\begin{aligned} \begin{bmatrix} V_{\alpha_k} \\ V_{\beta_k} \end{bmatrix} &= \sqrt{\frac{2}{3}} \begin{bmatrix} 1 & -1/2 & -1/2 \\ 0 & \sqrt{3}/2 & -\sqrt{3}/2 \end{bmatrix} \begin{bmatrix} V_{a\,k} \\ V_{b\,k} \\ V_{c_k} \end{bmatrix} \\ &= \sqrt{\frac{2}{3}} V_m \begin{bmatrix} \cos(\theta(kT)) \\ \sin(\theta(kT)) \end{bmatrix} + \begin{bmatrix} v_{\alpha_k} \\ v_{\beta_k} \end{bmatrix}, \end{aligned} \tag{3}$$

where the noise voltages $v_{\alpha_k} = \sqrt{\frac{2}{3}}\left(v_{a_k} - \frac{1}{2}v_{b_k} - \frac{1}{2}v_{c_k} \right)$ and $v_{\beta_k} = \sqrt{\frac{2}{3}}\left(\frac{\sqrt{3}}{2}v_{b_k} - \frac{\sqrt{3}}{2}v_{c_k} \right)$ are also zero-mean white Gaussian noise with common variance σ^2.

Let $A = \sqrt{\frac{2}{3}}V_m$, then a complex voltage V_k can be obtained from (3) as

$$\begin{aligned} V_k &= V_{\alpha_k} + jV_{\beta_k} \\ &= A\cos\left(\theta(kT)\right) + v_{\alpha_k} + j\left[A\sin\left(\theta(kT)\right) + v_{\beta_k}\right] \\ V_k &= Ae^{j\theta(kT)} + v_k \end{aligned} \tag{4}$$

Where $v_k = v_{\alpha_k} + jv_{\beta_k}$ is zero-mean complex Gaussian noise. Now, at time $(k+1)T$, the complex voltage is given by

$$V_{k+1} = Ae^{j\theta((k+1)T)} + v_{k+1}. \tag{5}$$

But,

$$\begin{aligned} \theta((k+1)T) &= \int_0^{(k+1)T} \omega(\tau)d\tau + \phi \\ &= \int_0^{kT} \omega(\tau)d\tau + \int_{kT}^{(k+1)T} \omega(\tau)d\tau + \phi, \\ &= \theta(kT) + \Delta\theta(T) \end{aligned} \tag{6}$$

where $\Delta\theta(T) \equiv \int_{kT}^{(k+1)T} \omega(\tau)d\tau$.

Hence, at time $(k+1)T$ the complex voltage model is given by

$$V_{k+1} = Ae^{j(\theta(kT)+\Delta\theta(T))} + v_{k+1}. \tag{7}$$

This model can also be represented in state-space form by defining the states at time kT as

$$\underline{\boldsymbol{x}}_k = \begin{bmatrix} x_{1k} \\ x_{2k} \end{bmatrix} \equiv \begin{bmatrix} e^{j\Delta\theta(T)} \\ Ae^{j\theta(kT)} \end{bmatrix}. \tag{8}$$

Thus, at time $(k+1)T$, we get

$$\begin{aligned} \underline{\boldsymbol{x}}_{k+1} &= \underline{\boldsymbol{f}}(\underline{\boldsymbol{x}}_k) + \underline{\boldsymbol{\eta}}_k \\ y_k &= h(\underline{\boldsymbol{x}}_k) + v_k \end{aligned}, \tag{9}$$

where

$$\begin{aligned}\boldsymbol{f}(\underline{\boldsymbol{x}}_k) &= \begin{bmatrix} e^{j\Delta\theta(T)} & Ae^{j\theta((k+1)T)} \end{bmatrix}^T \\ &= \begin{bmatrix} x_{1k} & x_{1k}\cdot x_{2k} \end{bmatrix}^T \\ h(\underline{\boldsymbol{x}}_k) &= x_{2k} = \begin{bmatrix} 0 & 1 \end{bmatrix}\begin{bmatrix} x_{1k} \\ x_{2k} \end{bmatrix}\end{aligned}, \quad (10)$$

$\underline{\boldsymbol{\eta}}_k$ is a complex zero-mean Gaussian noise vector with covariance matrix $\boldsymbol{Q}_k$ and v_k is a complex scalar zero-mean Gaussian noise with variance R_k^v.

The complex-valued signal state model of Eqs. (9) and (10) can be used to estimate the time-varying frequency of a sinusoidal signals corrupted with white Gaussian noise. Furthermore, it can be extended to represent sinusoidal signals containing harmonics.

3. STF-based master-slave UKF frequency estimator

The UKF is a powerful nonlinear estimator that works under the assumption that it is easier to approximate a Gaussian distribution than it is to approximate an arbitrary nonlinear function [27]. The UKF evaluates the nonlinear function with a minimal set of carefully selected sampling points distributed through $2n+1$ sigma points, where n is the number of states. These sigma points are based on a square root decomposition of the a priori covariance [27]. As in the EKF, the UKF uses a recursive algorithm that employs the system model, measurements, and known statistics of the noise.

Let us first consider the frequency estimation using only the master UKF [27]. Given that $n=2$, the UKF design procedure is now outlined.

Sigma Points Calculation in the k^{th} time instant:

$$\begin{aligned}&\underline{\boldsymbol{\chi}}_{0,k-1} = \hat{\underline{\boldsymbol{x}}}_{k-1} \\ &\underline{\boldsymbol{\chi}}_{i,k-1} = \hat{\underline{\boldsymbol{x}}}_{k-1} + \tau\left(\sqrt{\hat{\boldsymbol{P}}_{k-1}}\right)_i, \; i=1,2 \\ &\underline{\boldsymbol{\chi}}_{i+2,k-1} = \hat{\underline{\boldsymbol{x}}}_{k-1} - \tau\left(\sqrt{\hat{\boldsymbol{P}}_{k-1}}\right)_i, \; i=1,2\end{aligned} \quad (11)$$

where $\left(\sqrt{\hat{\boldsymbol{P}}_{k-1}}\right)_i$ is the i^{th} column of the sigma points covariance matrix $\sqrt{\hat{\boldsymbol{P}}_{k-1}} = \boldsymbol{M}_{k-1}$, $\boldsymbol{P}_{k-1} = \boldsymbol{M}_{k-1}\boldsymbol{M}_{k-1}^T$, $\tau = \sqrt{2+\lambda}$, and $\lambda = 2(\gamma^2 - 1)$. The parameter γ describes the spread of the i^{th} sigma point around the measurement estimate $\hat{\underline{\boldsymbol{x}}}_{k-1}$. If $\lambda > 0$, the points are scaled further from $\hat{\underline{\boldsymbol{x}}}_{k-1}$ and when $\lambda < 0$, the points are scaled towards $\hat{\underline{\boldsymbol{x}}}_{k-1}$. Moreover, the parameter $\gamma \in [10^{-4}, 1]$ is used to control the amount of higher-order nonlinearities around $\hat{\underline{\boldsymbol{x}}}_{k-1}$. The matrix $\hat{\boldsymbol{P}}_{k-1}$ is assumed positive definite. Therefore, its square root can be computed using the Cholesky decomposition to reduce computational time.

Time Update (Prediction):

$$\begin{cases} \underline{\boldsymbol{\chi}}_{i,k|k-1} = \underline{\boldsymbol{f}}(\underline{\boldsymbol{\chi}}_{i,k-1}), \; i=0,1,\cdots,4 \\ \hat{\underline{\boldsymbol{x}}}_{k|k-1} = \sum_{i=0}^{4} W_i^m \underline{\boldsymbol{\chi}}_{i,k|k-1} \\ \hat{\boldsymbol{P}}_{k|k-1} = \sum_{i=0}^{4} W_i^c \left[\underline{\boldsymbol{\chi}}_{i,k|k-1} - \hat{\underline{\boldsymbol{x}}}_{k|k-1}\right]\left[\underline{\boldsymbol{\chi}}_{i,k|k-1} - \hat{\underline{\boldsymbol{x}}}_{k|k-1}\right]^* + \boldsymbol{Q}_k \\ \gamma_{i,k|k-1} = h(\underline{\boldsymbol{\chi}}_{i,k|k-1}), \; i=0,1,\cdots,4 \\ \hat{y}_{k|k-1} = \sum_{i=0}^{4} W_i^m \gamma_{i,k|k-1} \end{cases} \quad (12)$$

Measurement Update:

$$\begin{cases} P_{y_k y_k} = \sum_{i=0}^{4} W_i^c \left|\gamma_{i,k|k-1} - \hat{y}_{k|k-1}\right|^2 + R_k \\ \boldsymbol{P}_{\underline{x}_k y_k} = \sum_{i=0}^{4} W_i^c \left[\underline{\boldsymbol{\chi}}_{i,k|k-1} - \hat{\underline{\boldsymbol{x}}}_{k|k-1}\right]\left[\gamma_{i,k|k-1} - \hat{y}_{k|k-1}\right]^* \\ \boldsymbol{K}_k = \boldsymbol{P}_{\underline{x}_k y_k}(P_{y_k y_k})^{-1} \\ \hat{\boldsymbol{P}}_k = \hat{\boldsymbol{P}}_{k|k-1} - \boldsymbol{K}_k P_{y_k y_k} \boldsymbol{K}_k^T \\ \hat{\underline{\boldsymbol{x}}}_k = \hat{\underline{\boldsymbol{x}}}_{k|k-1} + \boldsymbol{K}_k(y_k - \hat{y}_{k|k-1}) \end{cases}, \quad (13)$$

where the weights W_0^m, W_0^c, W_i^m, and W_i^c are defined by

$$\begin{aligned} W_0^m &= \frac{\lambda}{2+\lambda} \\ W_0^c &= \frac{\lambda}{2+\lambda} + (1 - \gamma^2 + \mu) \\ W_i^m &= W_i^c = \frac{1}{2(2+\lambda)}, \; i=1,\cdots,4 \end{aligned} \quad (14)$$

The constant μ is used to incorporate part of the prior knowledge of the statistics of $\underline{\boldsymbol{x}}_k$. We use $\mu = 2$, since it has been shown that $\mu = 2$ is optimal for Gaussian distributions [20].

Estimation performance can be further improved by tuning the state covariance matrix and the Kalman gain using the strong tracking properties of the Kalman filter [30].

As noted in [30,31], a STF can self-adaptively tune the error covariance matrix $\boldsymbol{P}_k$ and the corresponding Kalman gain $\boldsymbol{K}_k$ by introducing a "time-varying fading matrix". When the filter is linearized, this fading matrix is applied as follows:

$$\boldsymbol{P}_{k|k-1} = LMD_k \cdot \boldsymbol{F}_{k-1}\boldsymbol{P}_{k-1}\boldsymbol{F}_{k-1}^T + \boldsymbol{Q}_{k-1}, \quad (15)$$

where LMD is the so-called time-varying fading matrix and $LMD_k = diag[\lambda_{1_k}, \lambda_{2_k}, ..., \lambda_{n_k}]$ where $\lambda_{i_k} \geq 1 \;\; i = 1, 2, ..n$, are the fading factors and $\boldsymbol{F}_k$ is the system matrix of the linearized system dynamics $\underline{\boldsymbol{f}}(\underline{\boldsymbol{x}}_k)$ evaluated at a nominal operating point. $\boldsymbol{Q}_k$ is the process noise covariance matrix.

In so far as our system described by Eq. (10) is concerned, $n=2$ and the fading matrix can be calculated using the following algorithm:

$$\psi_k = y_k - \hat{y}_{k|k-1} \tag{16}$$

$$V_k = \begin{cases} \psi_0 \psi_0^T, & k = 0 \\ \dfrac{\rho V_{k-1} + \psi_k \psi_k^T}{1+\rho}, & k \geq 1 \end{cases} \tag{17}$$

$$N_k = V_k - \beta R_k - \boldsymbol{H}_k \boldsymbol{Q}_k \boldsymbol{H}_k^T \tag{18}$$

$$\boldsymbol{M}_k = \boldsymbol{H}_k \boldsymbol{F}_{k-1} \boldsymbol{P}_{k-1} \boldsymbol{F}_{k-1}^T \boldsymbol{H}_k^T \tag{19}$$

$$c_k = \frac{tr[N_k]}{\sum_{i=1}^{n} \alpha_i M_{ii,k}} \tag{20}$$

$$\lambda_{i_k} = \begin{cases} \alpha_i c_k & , \alpha_i c_k > 1 \\ 1 & , \alpha_i c_k \leq 1 \end{cases}, i = 1,2 \tag{21}$$

where ψ_k is the innovation, $\boldsymbol{H}_k$ is the matrix of the linearized measurement $h(\underline{\boldsymbol{x}}_k)$. R_k is the measurement noise covariance, the parameters ρ and β are the forgetting and weak factors, respectively. According to [30] the forgetting factor $\rho \in (0,1)$ and is commonly chosen to be 0.95 [30]. The weak factor β is greater than 1 for smoothing the estimation. $M_{ii,k}$'s are the diagonal components of $\boldsymbol{M}_k$. Finally, the coefficient values $\alpha_i \geq 1,\ i = 1,2$ are predetermined from prior knowledge of the system. If there is no prior knowledge about the system, $\alpha_i = 1,\ i = 1,2$.

Under the STF condition, the covariance matrix in Eq. (12) of the UKF is modified as follows:

$$\hat{\boldsymbol{P}}_{k|k-1} = LMD_k \cdot \sum_{i=0}^{4} W_i^c \left[\underline{\boldsymbol{\chi}}_{i,k|k-1} - \underline{\hat{\boldsymbol{x}}}_{k|k-1}\right]\left[\underline{\boldsymbol{\chi}}_{i,k|k-1} - \underline{\hat{\boldsymbol{x}}}_{k|k-1}\right]^* + \boldsymbol{Q}_k \tag{22}$$

where LMD_k is a 2 dimensional diagonal matrix.

3.1 Speed of Convergence

There is an inherent trade-off between speed of convergence and accuracy of the filter. If, as in the following example, the process noise covariance is underestimated, then the filter will take a long time to converge. Furthermore, if the process noise covariance is highly underestimated due to lack of knowledge of the system, the filter may be susceptible to divergence. Fig. 1 shows estimation performance for a linear change in frequency. We can see that without the STF condition the UKF diverges because of a poor selection of the process noise covariance $\boldsymbol{Q}$. However, the UKF filter under STF eventually converges to the actual signal. We can also see that for high β values the tracking ability becomes smoother at the price of slower convergence time. Furthermore, the lower the β values, the higher the sensitivity to changes. Therefore a compromise has to be made between the smoothness of the estimation and convergence time. This compromise can be less critical if we could successfully estimate the process noise covariance matrix $\boldsymbol{Q}_k$.

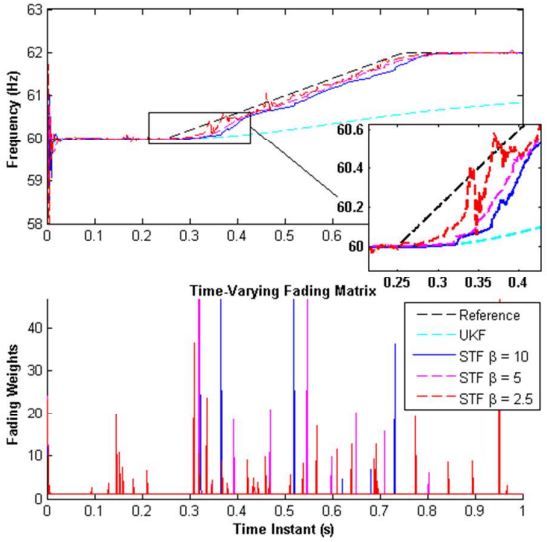

Fig. 1. *UKF under STF for different β values*

3.2 Sensitivity to Initial Conditions

Let us now examine how the UKF under STF performs for poorly chosen initial conditions. The comparison is made against UKF alone estimation. Fig. 2 shows estimation performance for a step change in frequency. We can see that the UKF does not converge to the true value due to the selected initial conditions. However, when we examine the UKF under STF we can see that the filter converges to the true value after the time-varying fading matrix LMD_k reaches unity.

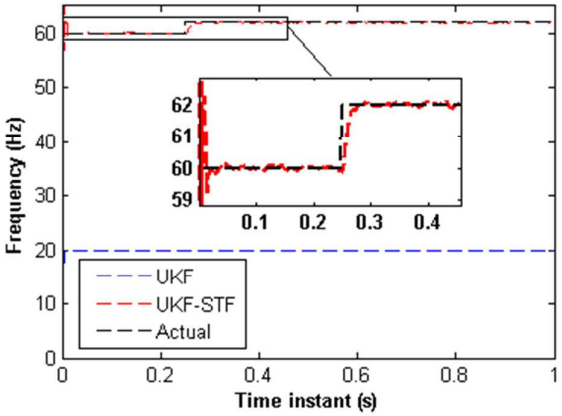

Fig. 2. *Filter performance under poorly chosen initial conditions*

3.3 Proposed approach

In real physical applications, the difference between the a-priori knowledge and the true state statistics is the major factor that degrades the filter's performance. Therefore, selecting appropriate covariance matrices ($\boldsymbol{Q}_k, R_k$) is of utmost importance in order to achieve the desired performance and stability of the UKF filter. To address this issue, we propose the use of a slave UKF to estimate the covariance in real time. Under the assumption that the process and measurement noises are Gaussian and white, one can safely assume that the covariance matrices $\boldsymbol{Q}_k$ and

R_k are diagonal matrices [27]. Then the estimation of the noise covariance can be simplified to the estimation of the diagonal elements.

The proposed adaptive frequency estimation scheme is shown in Fig. 3. It is composed of two UKF filters. At every time step, the master UKF estimates the states using the noise covariance obtained by the slave UKF, while the slave UKF estimates the noise covariance using the innovations generated by the master UKF.

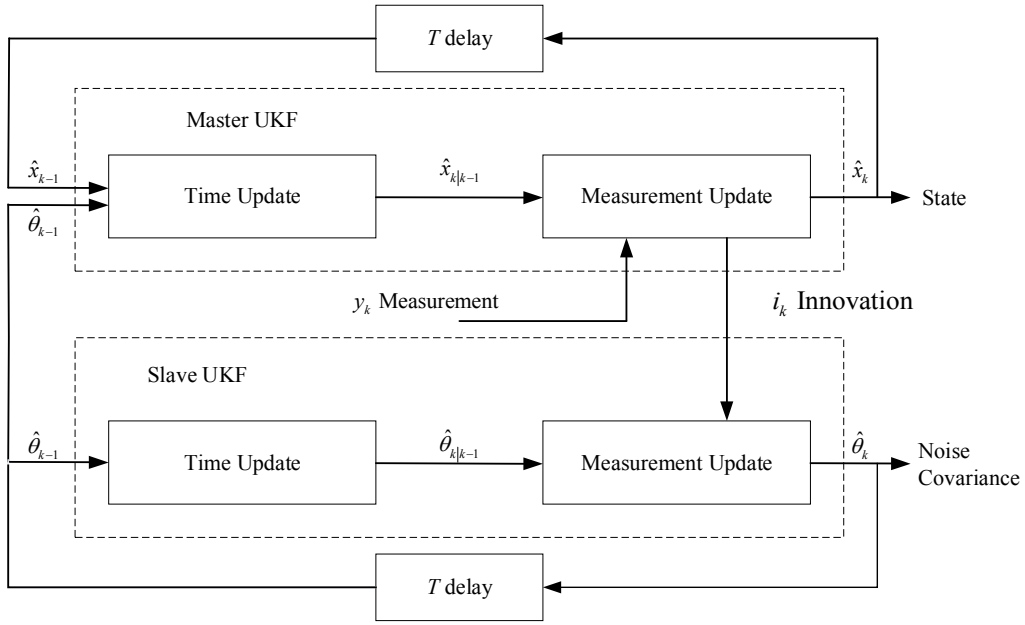

Fig. 3. *Proposed adaptive MS-UKF structure*

In this configuration, the slave UKF is used to estimate the measurement noise covariance R_k, and since it is a scalar, we let $\theta_k = R_k$. Now, if the dynamics of the parameter θ, namely, $f_\theta(\cdot)$, were known, then the time evolution of the parameter θ would be described by

$$\theta_k = f_\theta(\theta_{k-1}) + w_{\theta_k}. \tag{23}$$

On the other hand, if the dynamics of θ were unknown, as is the case herein, then several online parameter estimation methods based on particle filters principles such as expectation maximization (EM) algorithms and model averaging particle filters [32, 33] could be used to estimate θ. However, a simple model of the time evolution of θ can be built by introducing artificial dynamics to the parameter θ [32], i.e.

$$\theta_k = \theta_{k-1} + w_{\theta_k}, \tag{24}$$

where w_{θ_k} is a small artificial dynamic noise with variance Q^θ. When using this model, $f_\theta(\theta_{k-1}) = \theta_{k-1}$.

The measurement model for the estimation of θ is described by

$$s_k = h_\theta(\theta_k) + v_{\theta_k} = \theta_k + |i_k|^2 \tag{25}$$

where $i_k = y_k - \hat{y}_{k|k-1}$ is the innovation obtained by the master UKF and y_k is the physical measurement. The innovation is provided by the master UKF as an input to the slave UKF. The term $|i_k|^2$ is interpreted as a random noise (uncertainty) v_{θ_k} with variance R^θ. Clearly, v_{θ_k} is not Gaussian distributed. We choose the UKF to estimate the parameter θ because it still produces an unbiased estimate of it even when the noise is non-Gaussian [27] and to avoid the added computations due to resampling used by PFs.

The algorithm of the slave UKF is formulated in a similar manner as that of its master counterpart.

Slave: Sigma Points Calculation in the k^{th} time instant:

$$\begin{aligned}
\varphi_{0,k-1} &= \hat{\theta}_{k-1} \\
\varphi_{1,k-1} &= \hat{\theta}_{k-1} + \sigma\sqrt{\hat{P}_{\theta_{k-1}}} \\
\varphi_{2,k-1} &= \hat{\theta}_{k-1} - \sigma\sqrt{\hat{P}_{\theta_{k-1}}}
\end{aligned} \tag{26}$$

where $\sigma = \sqrt{\lambda_\theta + 1}$ and $\lambda_\theta = \delta^2 - 1$. The parameter δ is selected in a similar manner as γ in the master UKF.

Slave: Time Update (Prediction):

$$\begin{cases} \varphi_{i,k|k-1} = f_\theta(\varphi_{i,k-1}),\ i=0,1,2 \\ \hat{\theta}_{k|k-1} = \sum_{i=0}^{2} W_{\theta_i}^m \varphi_{i,k|k-1} \\ \hat{P}_{\theta_{k|k-1}} = \sum_{i=0}^{2} W_{\theta_i}^m \left|\varphi_{i,k|k-1} - \hat{\theta}_{k|k-1}\right|^2 + Q_{k-1}^\theta \\ \varsigma_{i,k|k-1} = h_\theta(\varphi_{k|k-1}),\ i=0,1,2 \\ \hat{s}_{k|k-1} = \sum_{i=0}^{2} W_{\theta_i}^m \varsigma_{i,k|k-1} \end{cases} \quad (27)$$

Slave: Measurement Update:

$$\begin{cases} P_{S_kS_k} = \sum_{i=0}^{2} W_{\theta_i}^c \left|\varsigma_{i,k|k-1} - \hat{s}_{k|k-1}\right|^2 + R_k^\theta \\ P_{\theta_kS_k} = \sum_{i=0}^{2} W_{\theta_i}^c \left|\varphi_{i,k|k-1} - \hat{\theta}_{k|k-1}\right|^2 \\ K_{\theta_k} = P_{\theta_kS_k}(P_{S_kS_k})^{-1} \\ \hat{P}_{\theta_k} = \hat{P}_{\theta_{k|k-1}} - K_{\theta_k} P_{S_kS_k} K_{\theta_k}{}^T \\ \hat{\theta}_k = \hat{\theta}_{k|k-1} + K_{\theta_k}(s_k - \hat{s}_{k|k-1}) \end{cases} \quad (28)$$

where Q^θ and R^θ are the slave's process and measurement noise covariances, respectively. The weights $W_{\theta_i}^c$ and $W_{\theta_i}^m$ can be calculated using a relation similar to that described by Eq. (14).

4. Simulation results

We assess performance of the proposed frequency estimation algorithm via computer simulation as follows: First, the EKF, UKF and MS-UKF are compared for different frequency changes and their average MSEs are computed using 100 independent runs. Next, the UKF under STF and MS-UKF under STF are compared for an underestimated and overestimated value of the measurement noise covariance R and their average MSEs are also computed using 100 independent runs.

Because we want to examine the filters under the same conditions without using optimal values of the measurement noise covariance, we have selected R such that it is both under and overestimated by a factor of 4. As was previously mentioned, the MS-UKF is able to estimate the process noise covariance and adapt the estimation to such uncertainty. Furthermore, since we do not have prior knowledge of the dynamics of R, we use the uncorrelated random walk model.

4.1. Performance Assessment

In order to evaluate the performance of the different estimators, we conduct three experiments where we introduce step, linear and nonlinear voltage frequency changes. All the estimators are subject to the same process and measurement noise and use the same voltage frequency measurement signal model described by (1)-(10). Finally, the plots that show the frequency tracking of the estimators over time are obtained at an SNR of 25 dB, using a sampling frequency of 1000 Hz.

***4.1.1** Experiment* 1**:** In this experiment the fundamental frequency of the sinusoidal signal undergoes a step change from 60 Hz to 59 Hz. Fig. 4(a) shows how well the MS-UKF, the ECKF, and the UKF estimators track the sudden change in frequency. We can see in this figure that the MS-UKF converges to within a small error of the actual frequency after about 0.05 seconds (approximately 50 samples), whereas the UKF and the EKF experience difficulties converging. Clearly, the MS-UKF produces more accurate estimates (much smaller ripples) than both the UKF and the EKF. The plot of Fig. 4(b) shows the tracking error for the step change in frequency of Fig. 4(a). This figure shows that the error between the actual frequency and that estimated by the MS-UKF is very small a short time after the step change. Table 1 shows the average MSE over 100 independent runs for a step change in frequency.

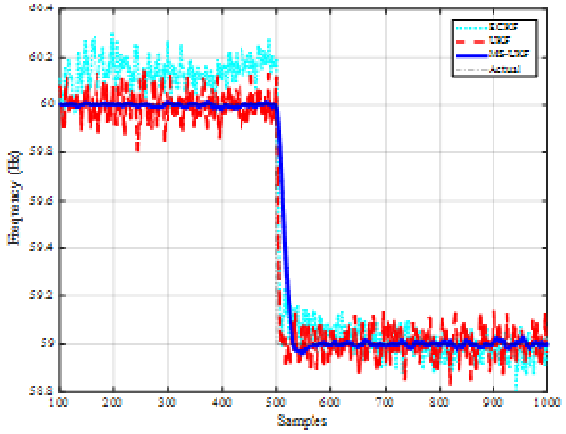

(a)

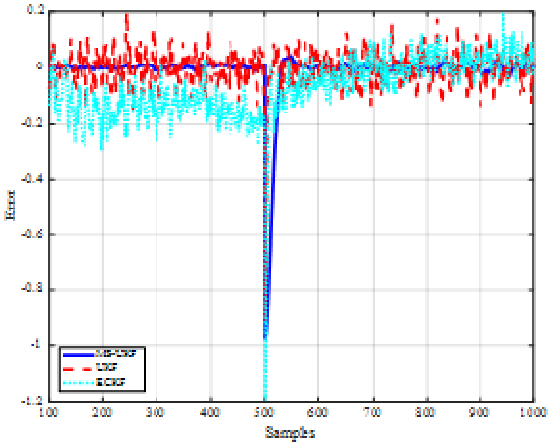

(b)

Fig. 4. *Estimator tracking of a frequency step change from 60 Hz to 59 Hz. (a) Actual and estimated frequency, (b) Tracking error*

Table 1. Mean MSE over 100 independent runs for a frequency step change

Frequency Step Variation MSE			
SNR	**ECKF**	**UKF**	**MS-UKF**
15	0.1839	0.1555	0.1200
20	0.1345	0.1111	0.0883
30	0.0759	0.0601	0.0450
40	0.0442	0.0318	0.0279
50	0.0267	0.0160	0.0112
60	0.0152	0.0075	0.0058

4.1.2 Experiment 2*:* The fundamental frequency of the sinusoidal signal undergoes a linear variation, namely, the instantaneous phase angle changes in a parabolic manner over a 0.3 seconds time interval.

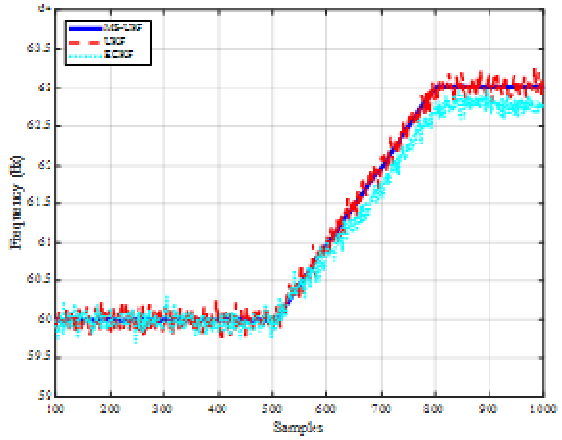

(a)

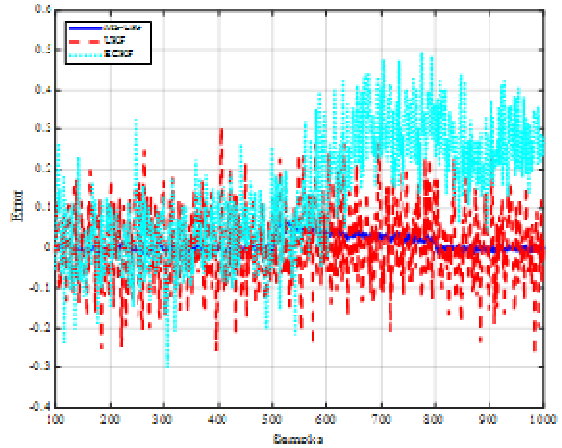

(b)

Fig. 5. *Estimator tracking of a linear frequency change from 60 Hz to 63 Hz. (a) Estimated frequency, (b) Tracking error*

Once again it can be seen in Figs. 5(a) and 5(b) that the MS-UKF is much better at tracking a linear frequency change than both the UKF and the EKF, i.e. the MS-UKF accurately tracks the frequency during the entire time with negligible error. Table 2 corroborates the observations made based on the plot.

Table 2. Mean MSE over 100 independent runs for linear frequency change

Linear Frequency Variation MSE			
SNR	**ECKF**	**UKF**	**MS-UKF**
15	1.883×10^{-01}	1.719×10^{-01}	7.030×10^{-02}
20	1.445×10^{-01}	1.304×10^{-01}	5.010×10^{-02}
30	7.380×10^{-02}	7.130×10^{-02}	2.240×10^{-02}
40	1.520×10^{-02}	1.450×10^{-02}	3.900×10^{-03}
50	8.300×10^{-03}	7.300×10^{-03}	1.900×10^{-03}
60	4.000×10^{-03}	3.000×10^{-03}	1.600×10^{-03}

4.1.3 Experiment 3: In this case the fundamental frequency of the sinusoidal signal is modulated by a small frequency component (nonlinear frequency change) starting at 0.38 seconds. Figs. 6(a) and 6(b) show the tracking performance of ECKF, UKF, and MS-UKF. It is clear from these figures that the MS-UKF tracks the modulated signal better than the other estimators. In fact, the MS-UKF starts tracking in about 0.02 seconds after the change occurs with a small error thereafter. The UKF performs better than the EKF, although both display a larger tracking error than the MS-UKF. Table 3 corroborates the visual results.

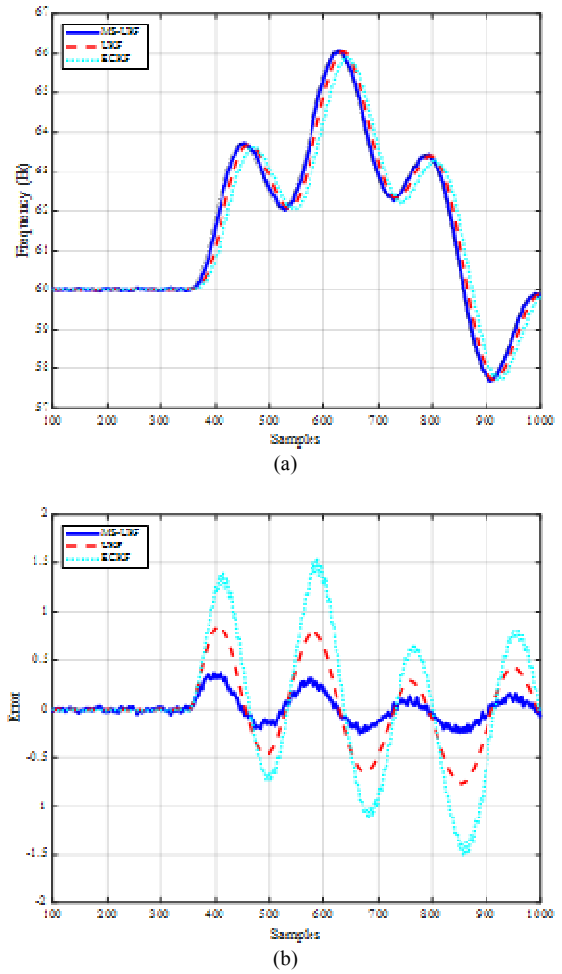

Fig. 6. *Estimator tracking of a nonlinear frequency change. (a) Estimated frequency, (b) Tracking error*

Table 3. MSE over 100 independent runs nonlinear frequency variations

Nonlinear Frequency Variation MSE			
SNR	**ECKF**	**UKF**	**MS-UKF**
15	0.4830	0.3889	0.3392
20	0.2993	0.2482	0.2161
30	0.1314	0.1043	0.0833
40	0.0534	0.0354	0.0272
50	0.0239	0.0106	0.0095
60	0.0117	0.0048	0.0034

Although the MS-UKF performs better than the other estimators, the problem of initial conditions may still an issue when it comes to convergence. As it was pointed out in section 3, all these filters may diverge if the initial conditions are poorly chosen.

4.2 UKF-STF vs MS-UKF-STF

By implementing the STF condition on the filters, we can effectively desensitize the estimators with respect to initial conditions. As seen in Fig. 1, the β values can be tuned to work well with a certain amount of uncertainty, i.e. our initial guess of measurement noise covariance R. This is an inherent weakness when we do not know what the value of R is or if it changes with time. To assess frequency estimation performance under ST conditions, the simulations assume an under and over estimated R by a factor of 4. Tables 4 through 6 show the improvement that can achieved if we know the value of the process noise and adapt to its changes.

Table 4. Mean MSE over 100 independent runs for frequency step

Frequency Steps Variation MSE			
SNR	**UKF-STF (4*R)**	**UKF-STF (1/4*R)**	**MS-UKF**
15	8.10×10^{-01}	5.10×10^{-01}	4.50×10^{-01}
20	7.68×10^{-01}	3.36×10^{-01}	3.25×10^{-01}
30	5.60×10^{-01}	1.66×10^{-01}	1.84×10^{-01}
40	1.92×10^{-01}	8.36×10^{-02}	9.33×10^{-02}
50	9.85×10^{-02}	5.44×10^{-02}	6.10×10^{-02}
60	5.37×10^{-02}	4.08×10^{-02}	4.60×10^{-02}

Table 5. Mean MSE over 100 independent runs for linear frequency change

Linear Frequency Variation MSE			
SNR	**UKF-STF (4*R)**	**UKF-STF (1/4*R)**	**MS-UKF**
15	4.16×10^{-02}	2.71×10^{-02}	3.58×10^{-02}
20	2.31×10^{-02}	1.54×10^{-02}	2.03×10^{-02}
30	7.70×10^{-03}	5.20×10^{-03}	5.30×10^{-03}
40	2.50×10^{-03}	2.40×10^{-03}	1.90×10^{-03}
50	9.00×10^{-04}	1.20×10^{-03}	8.00×10^{-04}
60	3.00×10^{-04}	7.00×10^{-04}	3.00×10^{-04}

Table 6. Mean MSE over 100 independent runs for modulated frequency

Nonlinear Frequency Variation MSE			
SNR	**UKF-STF (4*R)**	**UKF-STF (1/4*R)**	**MS-UKF**
15	3.83×10^{-01}	1.50×10^{-01}	1.82×10^{-01}
20	2.14×10^{-01}	6.39×10^{-02}	1.12×10^{-01}
30	6.61×10^{-02}	2.37×10^{-02}	3.34×10^{-02}
40	2.13×10^{-02}	8.70×10^{-03}	1.19×10^{-02}
50	7.00×10^{-03}	4.10×10^{-03}	4.30×10^{-03}
60	2.30×10^{-03}	1.60×10^{-03}	1.60×10^{-03}

As can be seen in Figs. 7 through 9, the MS-UKF-STF outperforms the UKF-STF regardless of the value of the measurement noise covariance R because the former provides a more accurate estimation of the measurement noise covariance. Specifically, the MS-UKF-STF estimator has a more robust frequency tracking performance in terms of convergence than the UKF-STF estimator.

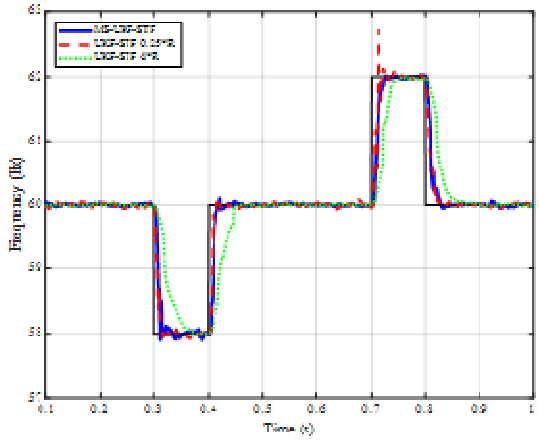

(a)

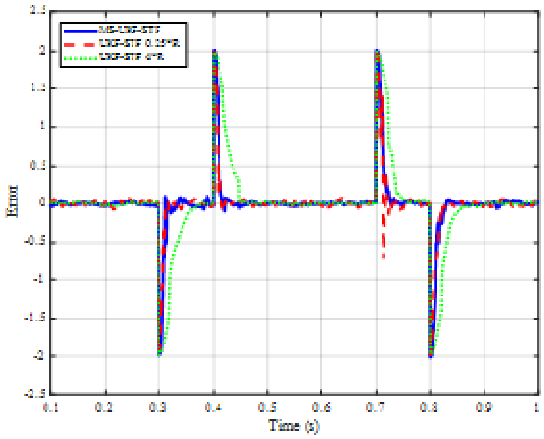

(b)

Fig. 7. *MS-UKF-STF and UKF-STF tracking for frequency step changes. (a) Estimated frequency, (b) Tracking error*

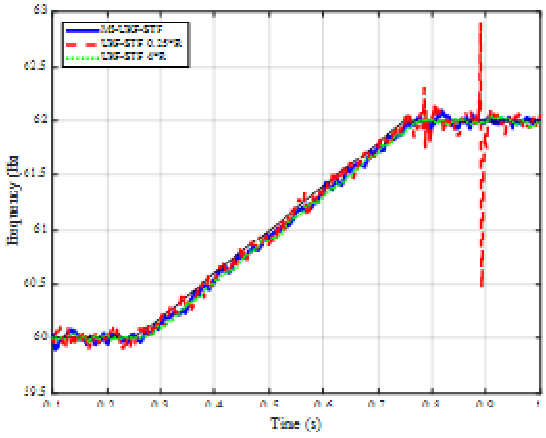

(a)

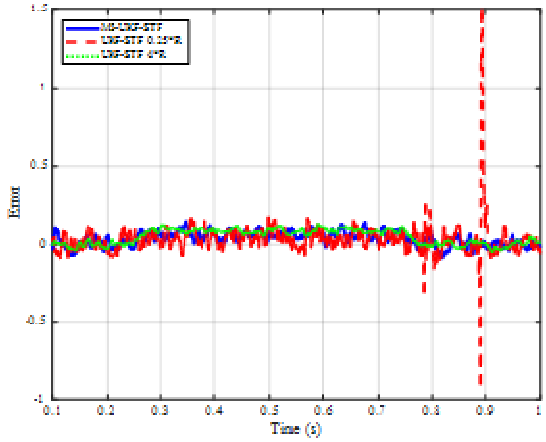

(b)

Fig. 8. *MS-UKF-STF and UKF-STF tracking for a linear frequency change. (a) Estimated frequency, (b) Tracking error*

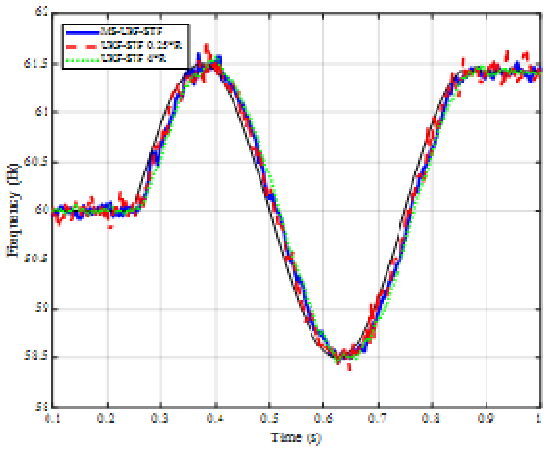

(a)

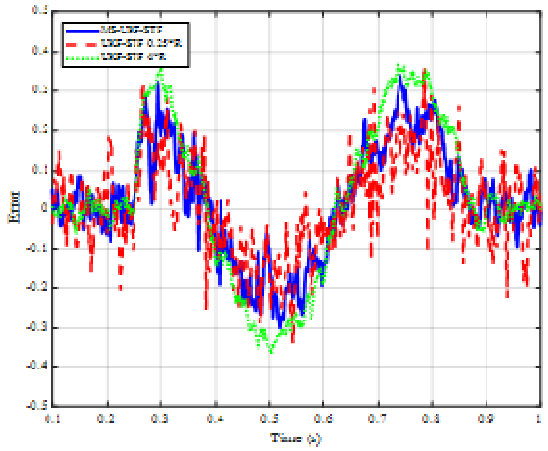

(b)

Fig. 9. *MS-UKF-STF and UKF-STF tracking for a non-linear frequency change. (a) Estimated frequency, (b) Tracking error*

5. Conclusions

In this paper, an adaptive frequency estimation algorithm based on a two-UKF structure is presented. The "master" UKF filter which is modified to operate under STF condition is used to estimate the frequency and the "slave" UKF filter is used to estimate the measurement noise covariance. Extensive computer simulations were run for different frequency variation scenarios and varying levels of noise to determine the performance of the proposed estimation approach. The proposed algorithm produced very good results even for voltage signals contaminated with significant levels of noise and with large abrupt changes in frequency.

6. References

[1] Jones, D.: 'Estimation of power system parameters,' IEEE Trans. Power Syst., 2004, 19, (4), pp. 1980–1989.

[2] Kamwa, I., Pradhan, A. K. and Joos, G.: 'Adaptive phasor and frequency- tracking schemes for wide-area protection and control,' IEEE Trans. Power Delivery, 2011, 26, (2), pp. 744–753.

[3] Roscoe, A. J., Burt, G. M. and McDonald, J. R.: 'Frequency and fundamental signal measurement algorithms for distributed control and protection applications,' IET Gen. Trans. Dist., 2009, 3, (5), pp. 485- 495.

[4] Kusljevic, M. D.: 'A simple recursive algorithm for simultaneous magnitude and frequency estimation,' IEEE Trans. Instrum. Measur., 2008, 57, (6), pp. 1207-1214.

[5] Xia, Y, Douglas, S. C. and Mandic, D. P.: 'Adaptive frequency estimation in smart grid applications: Exploiting noncircularity and Widely Linear Adaptive Estimators,' IEEE Signal Processing Magazine, 2012, 29, (5), pp. 44-54.

[6] Hancke, G. P.: 'The optimal frequency estimation of a noisy sinusoidal signal,' IEEE Transactions on Instrumentation and Measurement, 1990, 39, (6), pp. 843 - 846.

[7] Aghazadeh, R., Lesani, H., Sanaye-Pasand, M. and Ganji, B.: 'New technique for frequency and amplitude estimation of power system signals,' IEE Proceedings, Gen., Trans. Dist., 2005, 152, (3), pp. 435 -440.

[8] Park, S. Y., Song, Y. S., Kim, H. J., and Park, J.: 'Improved method for frequency estimation of sampled sinusoidal signal without iteration,' IEEE Transactions on Instrumentation and Measurement, 2011, 60, (8), pp. 2828-2834.

[9] Reza, M. S., Ciobotaru, M., and Agelidis, V. G.: 'A recursive DFT based technique for accurate estimation of grid voltage frequency,' Proceedings of the IECON – 39th Annual Conference, 2013 pp. 6420 – 6425.

[10] Ren, J. and Kezunovic, M.: 'A hybrid method for power system frequency estimation,' IEEE Transactions on Power Delivery, 2012, 27, (3), pp. 1252-1259.

[11] Fan, L. and Qi, G.: 'A new synthetic frequency estimation method of sinusoid based and interpolated FFT,' Proc. Fifth Int. Conference on Instrumentation and Measurement, Computer, Communication and Control, 2015, pp. 1725-1729.

[12] Pradhan, A. K., Routray, A., and Basak, A.: 'Power system frequency estimation using least mean square technique,' IEEE Transactions on Power Delivery, 2005, 20, (3), pp. 1812-1816.

[13] Kušljević, M. D.: 'On LS-based power frequency estimation algorithms,' IEEE Transactions on Instrumentation and Measurement, 2013, 62, (7), pp. 2020-2028.

[14] Xia, Y., Blazic, Z., and Mandic, D. P.: 'Complex-valued least squares frequency estimation for unbalanced power systems,' IEEE Transactions on Instrumentation and Measurement, 2015, 64, (3), pp. 638-648.

[15] Chudamani, R., Vasudevan, K. and Ramalingam, C.S.: 'Real-time estimation of power system frequency using nonlinear least squares,' IEEE Trans. on Power Delivery, 2009, 24, (3), pp. 1021-1028.

[16] Cheng, C-I. and Chang, G. W.: 'An efficient Prony-based solution procedure for tracking of power system voltage variations,' IEEE Transactions on Industrial Electronics, 2013, 60, (7), pp. 2681-2688.

[17] He, Z., Fu, L., Han, W., Mai, R., and Dong, Z. Y.: 'Precise algorithm for frequency estimation under dynamic and step-change conditions,' IET Science, Measurement and Technology, 2015, 9, (7), pp. 842-851.

[18] Hwang, J. K. and Markham, P. N.: 'Power system frequency estimation by reduction of noise using three digital filters,' IEEE Transactions on Instrumentation and Measurement, 2015, 63, (2), pp. 402-409.

[19] Yang, B., Peng, X. Y., Zheng, W. F., and Liu, S.: 'Optimal orthogonal subband fusion for online power system frequency estimation,' Electronic Letters, 2016, 52, (5), pp. 390-392.

[20] Xia, Y. and Mandic, D. P.: 'Widely linear adaptive frequency estimation of unbalanced three-phase power systems,' IEEE Transactions on Instrumentation and Measurement, 2012, 61, (1), pp. 74-83.

[21] Arulampalam, M. S., Maskell, S., Gordon, N., and Clapp, T.: 'A tutorial on particle filters for online nonlinear/non-Gaussian Bayesian tracking,' IEEE Trans. on Signal Processing, 2002, 50, (2), pp. 174-188.

[22] Ho, Y. C. and Lee, R. C. K.: 'A Bayesian approach to problems in stochastic estimation and control,' *IEEE Trans. on Automatic Control*, 1964, 9, (4) pp. 333-339.

[23] Suwantong, R., Bertrand, S., Dumur, D., and Beauvois, D.: 'Stability analysis and robustness assessment of deterministic and stochastic moving horizon estimators,' IEEE 55th Conference on Decision and Control, 2016, pp. 2900-2905.

[24] Mallick, M. La Scala, B., Ristic, B., Kirubarajan, T., and Hill, J.: 'Comparison of filtering algorithms for ground target tracking using space-based GMTI radar,' 18th International Conference on Information Fusion, 2015, pp. 1672-1679.

[25] Wiltshire, R., Ledwich, G., and O'Shea, P.: 'A Kalman filtering approach to rapidly detecting modal changes in power systems,' IEEE Trans. Power Syst., 2007, 22, (4), pp. 1698–1706.

[26] Huang, C.-H., Lee, C.-H., Shih, K.-J., and Wang, Y.-J.: 'A robust technique for frequency estimation of distorted signals in power systems,' IEEE Trans. Instrum. Meas., 2010, 59, (8), pp. 2026–2036.

[27] Julier, S. J. and Uhlmann, J. K.: 'Unscented filtering and nonlinear estimation,' Proceedings of the IEEE, 2004, 92, (3), pp. 401-422.

[28] Jian, Z., Swain, A., Nair, N. K. C., and Liu, J. J.: 'Estimation of power quality using an unscented Kalman filter,' TENCON 2007 - 2007 IEEE Region 10 Conference, 2007, pp. 1-4.

[29] Regulski, P. and Terzija, V.: 'Estimation of frequency and fundamental power components using an unscented Kalman filter,' IEEE Transactions on Instrumentation and Measurement, 2012, 61, (4), pp. 952-962.

[30] Narasimhappa, M., Sabat, S. L., and Nayak, J.: 'Adaptive sampling strong tracking scaled unscented Kalman filter for denoising the fibre optic gyroscope drift signal,' IET Science, Measurement and Technology, 2015, 9, (3), pp. 241-249.

[31] Li, H.: 'Applications of strong tracking filter in power system dynamic state estimation,' Proc. International Conference on Sustainable Power Generation and Supply, 2012, pp. 1-5.

[32] Andrieu, C., Doucet, A., Singh, S. S., and Tadić, V. B.: 'Particle methods for change detection, system identification, and control,' Proceedings of the IEEE, 2004, 92, (3), pp. 423-438.

[33] Martino, L., Read, J., Elvira, V., and Louzada, F.: 'Cooperative Parallel Particle Filters for on-Line Model Selection and Applications to Urban Mobility,' Digital Signal Processing, 2017, 60, p. 172-185.